

SEMI-ANNUAL PROGRESS REPORT

ON

DISTRIBUTED ACTIVE CONTROL

OF

LARGE FLEXIBLE SPACE STRUCTURES
(Grant # NAG 5-749)

Submitted by

✓
Dr. Charles C. Nguyen, Principal Investigator
Dr. Amr Baz, Principal Investigator
The Catholic University of America
Washington, D. C. 20064

to

Dr. Joseph V. Fedor Code 712
Space Technology Division
Goddard Space Flight Center
Greenbelt, Maryland 20771

November 1986

TABLE OF CONTENTS

	PAGE
Summary	
Symbols and Notations	
1. Introduction	4
2. Updated Research	5
3. Modeling of The Polar Platform	16
4. Project Research Results	16
5. Current and Future Research	20
6. Conclusion	21
References	
Figures and Tables	

SUMMARY

This progress report summarizes the research work performed at the Catholic University of America on the research grant entitled "Distributed Active Control of Large Flexible Space Structures," funded by NASA/Goddard Space Flight Center, under the grant number NAG 5-749, during the period of March 15, 1986 to September 15, 1986.

In this report we first update the research work relevant to the project. Then the research accomplished during the above period will be stated. The report is then concluded by a discussion of current and future research work.

SYMBOLS AND NOTATION

1. $\text{bd}(M_1; M_2; \dots; M_N) = \begin{bmatrix} M_1 & 0 & \dots & 0 \\ 0 & M_2 & \dots & 0 \\ \cdot & \cdot & & \cdot \\ \cdot & \cdot & & \cdot \\ 0 & 0 & & M_N \end{bmatrix}$

2. $M^T =$ Transpose of the matrix M

3. $0_{m \times n} =$ an $(m \times n)$ zero matrix

4. $I_n =$ an $(n \times n)$ identity matrix

5. $\dot{x}(t) = \frac{d}{dt} x(t)$

1. Introduction

The advent of a space transportation system, such as the space shuttle makes it possible to conceive of very large satellites and spacecraft which could be carried into space and deployed, assembled, or constructed there for such diverse purposes as communications, surveillance, astronomy, space exploration, and electric power generation [2]. These large space structures (LSS) concepts range from central rigid bodies, to the solar electric propulsion spacecraft and the generic polar platform. Two control problems for LSS are attitude control and shape control [24]. The former involves maintaining a given orientation of the spacecraft, e.g., with respect to the sun or earth; the latter involves maintaining the shape of critical structures of LSS. LSS are distributed parameter systems that possess many low resonant frequencies and have very stringent requirements for shape, orientation, alignment, vibration suppression and pointing accuracy. These requirements lead the control designers to the concept of active control of LSS with various sensors and actuators located about the structure and operating through on-line computer controllers to tailor the performance and behavior of the system.

There has been considerable interest in the area of active control of LSS [1]-[24]. A number of control schemes were proposed for large flexible space structure (LFSS), but they all represent one form or another of modal control [11]. Two main modal control schemes are the coupled Modal Control and Independent Modal Space Control (IMSC). The former employs an active controller consisting of a state estimator and a state feedback law; the latter controls each mode independently by means of the modal filter [13].

In this report we first update the research in active control of LFSS to provide a mathematical framework for the project. Then the modelling of a generic polar platform is developed using finite element method. After that some project research results are presented. We then discuss the current and future research effort. A conclusion will summarize the report.

2. Updated Research

In this section we first present the mathematical description of large space structures (LSS) and then discuss the two main control schemes for this type of structures.

2.1 Mathematical Description of LSS

The LSS may be described as a continuum by the following partial differential equations

$$M(P) \frac{\partial^2 u(P,t)}{\partial t^2} + L u(P,t) = f(P,t) \quad (2.1)$$

where $u(P,t)$ = displacement of an arbitrary point \underline{P}

L = Linear differential self-adjoint operator of order $2p$, expressing the system stiffness.

$M(P)$ = distributed mass

$f(P,t)$ = distributed control force

Equation (2.1) must be satisfied at every point P in the domain D . The displacement of $u(P,t)$ is subject to the boundary conditions

$$B_i u(P,t) = 0 \quad \text{for } i=1,2,\dots,p \quad (2.2)$$

where B_i are linear differential operator of order ranging from 0 to $(2p-1)$.

The associated eigenvalue problem is formulated by

$$L \phi_r(P) = \lambda_r M(P) \phi_r(P) \quad (2.3)$$

for $r=1,2,\dots,\infty$

with the boundary conditions

$$B_i \phi_r(P) = 0 \quad (2.4)$$

for $i=1,2,\dots,p; r=1,2,\dots,\infty$

where λ_r is the r th eigenvalues and $\phi_r(P)$ is the eigenfunction associated with λ_r . Sometimes $\phi_r(P)$ is called the mode shape.

Equations (2.3) and (2.4) can be solved to obtain the solutions of λ_r and ϕ_r and in addition, if the operator L is positive definite, then all eigenvalues are positive. The mode frequency (or natural frequency) is defined as

$$\omega_r = (\lambda_r)^{\frac{1}{2}}; r=1,2,\dots \quad (2.5)$$

using expansion theorem [11], the solution of $u(P,t)$ can be obtained as

$$u(P,t) = \sum_{r=1}^{\infty} \phi_r(P) u_r(t) \quad (2.6)$$

where $u_r(t)$ satisfies

$$\ddot{u}_r(t) + \omega_r^2 u_r(t) = f_r(t) \quad (2.7)$$

for $r=1,2,\dots$

and

$$f_r(t) = \int_D \phi_r(P) f(P,t) dD \quad (2.8)$$

In practice, the infinite series in (2.6) is truncated as

$$u(P,t) = \sum_{r=1}^M \phi_r(P) u_r(t) \quad (2.9)$$

where M is chosen to be sufficiently large so that $u(P,t)$ can be represented with good fidelity.

Since M may be quite large, it is not reasonable to control all M modes. Hence we select N modes to control. These N modes are called Controlled Modes. The remaining R modes ($R = M-N$) are called Residual Modes (uncontrolled modes).

Equation (2.7) can be transformed into the state equation form as follows

$$\dot{x}_C(t) = A_C x_C(t) + f_C(t) \quad (2.10)$$

$$\dot{x}_R(t) = A_R x_R(t) + f_R(t) \quad (2.11)$$

where $x_C(t) = [\dot{u}_1 \ \dot{u}_2 \ \dots \ \dot{u}_N \ u_1 \ u_2 \ \dots \ u_N]^T$ (2.12)

$$x_R(t) = [\dot{u}_{N+1} \ \dot{u}_{N+2} \ \dots \ \dot{u}_M \ u_{N+1} \ u_{N+2} \ \dots \ u_M]^T \quad (2.13)$$

$$f_C = [f_1 \ f_2 \ \dots \ f_N \ 0_{1 \times N}]^T \quad (2.14)$$

$$f_R = [f_{N+1} \ f_{N+2} \ \dots \ f_M \ 0_{1 \times R}]^T \quad (2.15)$$

$$A_C = \begin{bmatrix} 0_{N \times N} & | & \text{bd}(-\omega_1^2; -\omega_2^2; \dots; -\omega_N^2) \\ \hline I_N & & 0_{N \times N} \end{bmatrix} \quad (2.16)$$

$$A_R = \begin{bmatrix} 0_{R \times R} & | & \text{bd}(-\omega_{N+1}^2; \omega_{N+2}^2; \dots; \omega_M^2) \\ \hline I_R & & 0_{R \times R} \end{bmatrix} \quad (2.17)$$

Discrete Actuators: Since it is impossible to implement distributed control forces, the distributed control force $f(P,t)$ is realized by k discrete point force actuators

$$f(P,t) = \sum_{i=1}^k \delta(P-P_i) F_i(t) \quad (2.18)$$

where $\delta(P-P_i)$ is a spatial Dirac Delta function.

Substituting (2.18) into (2.8) yields

$$f_r(t) = \sum_{i=1}^k \phi_r(P_i) F_i(t); \quad r=1,2,\dots \quad (2.19)$$

Now using (2.19) we obtain

$$f_C(t) = B_C F(t) \quad (2.20)$$

$$\text{and } F_R(t) = B_R F(t) \quad (2.21)$$

$$B_C = \begin{bmatrix} \phi_1(P_1) & \phi_1(P_2) & \dots & \phi_1(P_k) \\ \phi_2(P_1) & \phi_2(P_2) & \dots & \phi_2(P_k) \\ \vdots & \vdots & & \vdots \\ \phi_N(P_1) & \phi_N(P_2) & \dots & \phi_N(P_k) \\ \hline & & & 0_{N \times k} \end{bmatrix} \quad (2.22)$$

$$B_R = \begin{bmatrix} \phi_{N+1}(P_1) & \phi_{N+1}(P_2) & \dots & \phi_{N+1}(P_k) \\ \phi_{N+2}(P_1) & \phi_{N+2}(P_2) & \dots & \phi_{N+2}(P_k) \\ \vdots & \vdots & & \vdots \\ \phi_M(P_1) & \phi_M(P_2) & \dots & \phi_M(P_k) \\ \hline & & & 0_{M \times k} \end{bmatrix} \quad (2.23)$$

$$\text{and } F(t) = [F_1 \ F_2 \ \dots \ F_k]^T \quad (2.24)$$

Discrete Sensors: Suppose there are s discrete sensors consisting of p velocity sensors, located at p locations $P_{v1}, P_{v2}, \dots, P_{vp}$ and q displacement sensors, located at q locations $P_{D1}, P_{D2}, \dots, P_{Dq}$. Using (2.9) we can express the velocity sensor output as

$$y_j = \dot{u}(P_{Vj}, t) = \sum_{r=1}^M \phi_r(P_{Vj}) \dot{u}_r(t) \quad (2.25)$$

for $j = 1, 2, \dots, p$, and the displacement sensor output as

$$y_{p+j} = u(P_{Dj}, t) = \sum_{r=1}^M \phi_r(P_{Dj}) u_r(t) \quad (2.26)$$

for $j = 1, 2, \dots, q$.

If we define the sensor output vector as

$$y(t) = [y_1 \ y_2 \ \dots \ y_p \ y_{p+1} \ y_{p+2} \ \dots \ y_{p+q}]^T, \quad (2.27)$$

then using (2.25) and (2.26), we can write

$$y(t) = C_C x_C(t) + C_R x_R(t) \quad (2.28)$$

where

$$C_C = bd[C_{CV} \ C_{CD}] \quad (2.29)$$

$$C_R = bd[C_{RV} \ C_{RD}] \quad (2.30)$$

and

$$C_{CV} = \begin{bmatrix} \phi_1(P_{V1}) & \phi_2(P_{V1}) & \dots & \phi_N(P_{V1}) \\ \phi_1(P_{V2}) & \phi_2(P_{V2}) & \dots & \phi_N(P_{V2}) \\ \vdots & \vdots & & \vdots \\ \phi_1(P_{Vp}) & \phi_2(P_{Vp}) & \dots & \phi_N(P_{Vp}) \end{bmatrix} \quad (2.31)$$

$$C_{CD} = \begin{bmatrix} \phi_1(P_{D1}) & \phi_2(P_{D1}) & \dots & \phi_N(P_{D1}) \\ \phi_1(P_{D2}) & \phi_2(P_{D2}) & \dots & \phi_N(P_{D2}) \\ \vdots & \vdots & & \vdots \\ \phi_1(P_{Dq}) & \phi_2(P_{Dq}) & \dots & \phi_N(P_{Dq}) \end{bmatrix} \quad (2.32)$$

$$C_{RV} = \begin{bmatrix} \phi_{N+1}(P_{V1}) & \phi_{N+2}(P_{V1}) & \dots & \phi_M(P_{V1}) \\ \phi_{N+1}(P_{V2}) & \phi_{N+2}(P_{V2}) & \dots & \phi_M(P_{V2}) \\ \vdots & \vdots & & \vdots \\ \phi_{N+1}(P_{Vp}) & \phi_{N+2}(P_{Vp}) & \dots & \phi_M(P_{Vp}) \end{bmatrix} \quad (2.33)$$

$$C_{RD} = \begin{bmatrix} \phi_{N+1}^{(P_{D1})} & \phi_{N+2}^{(P_{D1})} & \dots & \phi_M^{(P_{D1})} \\ \phi_{N+1}^{(P_{D2})} & \phi_{N+2}^{(P_{D2})} & \dots & \phi_M^{(P_{D2})} \\ \vdots & \vdots & & \vdots \\ \phi_{N+1}^{(P_{Dq})} & \phi_{N+2}^{(P_{Dq})} & \dots & \phi_M^{(P_{Dq})} \end{bmatrix}$$

The development in this section can be now summarized by the following modal state equation in matrix form

$$\begin{bmatrix} \dot{x}_C \\ \dot{x}_R \end{bmatrix} = \begin{bmatrix} A_C & 0 \\ 0 & A_R \end{bmatrix} \begin{bmatrix} x_C \\ x_R \end{bmatrix} + \begin{bmatrix} B_C \\ B_R \end{bmatrix} F(t) \quad (2.34)$$

$$y(t) = [C_C \quad C_R] \begin{bmatrix} x_C \\ x_R \end{bmatrix} \quad (2.35)$$

2.2 The Coupled Modal Control Scheme

In this scheme, the active controller consists of two parts:

a) a state estimator that accepts the sensor output $y(t)$ and produces an estimate $\hat{x}_C(t)$ of the controlled state $x_C(t)$ and

b) a linear state feedback control law that multiplies the estimated controlled state $\hat{x}_C(t)$ by constant gain to produce the actuator input $F(t)$.

The state estimator can be of the Luenberger type that is described by [15]

$$\dot{\hat{x}}_C(t) = (A_C - G_C C_C) \hat{x}_C(t) + B_C F(t) + G_C y(t) \quad (2.36)$$

The state estimator error is defined as

$$e_C(t) = \hat{x}_C(t) - x_C(t) \quad (2.37)$$

Therefore

$$\dot{e}_C(t) = \dot{\hat{x}}_C(t) - \dot{x}_C(t) = (A_C - G_C C_C) e_C(t) + G_C C_R x_R(t) \quad (2.38)$$

The linear state feedback law is defined by

$$F(t) = K_C \hat{x}_C(t) \quad (2.39)$$

Now substituting (2.39) into (2.34) and (2.38), we obtain the composite state equation as follows:

$$\begin{bmatrix} \dot{x}_C(t) \\ \dot{e}_C(t) \\ \dot{x}_R(t) \end{bmatrix} = \begin{bmatrix} A_C + B_C K_C & B_C K_C & 0 \\ 0 & A_C - G_C C_C & G_C C_R \\ B_R K_C & B_R K_C & A_R \end{bmatrix} \begin{bmatrix} x_C(t) \\ e_C(t) \\ x_R(t) \end{bmatrix} \quad (2.40)$$

The objective of the couple modal control scheme is to select K_C and G_C such that the composite system (2.40) is asymptotically stable. In (2.40) the

control spillover is represented by B_R and the observation spillover is represented by C_R . The coupled modal control scheme is illustrated in Figure 1.

2.3 The Independent Modal Space Control Scheme (IMSC)

The IMSC scheme was developed by Meirovitch and others [10] to control each mode independently. First an auxiliary variable $V_r(t)$ is defined by

$$v_r(t) = 1/\omega_r \dot{u}_r(t) \quad (2.41)$$

Therefore using (2.7) we can write

$$\dot{v}_r(t) = 1/\omega_r \ddot{u}_r(t) = -\omega_r^2 u_r(t) + f_r(t) \quad (2.42)$$

Now using (2.41) and (2.42), we obtain

$$\dot{x}_r(t) = A_r x_r(t) + W_r \quad (2.43)$$

where

$$A_r = \begin{bmatrix} 0 & \omega_r \\ -\omega_r & 0 \end{bmatrix} \quad (2.44)$$

$$W_r = [0 \quad f_r/\omega_r]^T \quad (2.45)$$

$$\text{and } x_r = [u_r \quad v_r]^T \quad (2.46)$$

The essence of the IMSC is to choose W_r such that W_r depends only on ω_r alone:

$$W_r = W_r(\omega_r) \quad (2.47)$$

The optimal design of W_r was discussed in [12].

Modal Filter; To implement the IMSC scheme, the modal displacements $u_r(t)$ and modal velocities $\dot{u}_r(t)$ are required. A device, called modal filter accepts the measurements of displacement $u(P,t)$ and velocity $\dot{u}(P,t)$ at every point P at all time and produces the modal displacement $u_r(t)$ and

modal velocity $u_r(t)$. The mathematical representation of a modal filter is given by

$$u_r(t) = \int_D M(P) \phi_r(P) u(P,t) dD \quad (2.48)$$

$$\dot{u}_r(t) = \int_D M(P) \phi_r(P) \dot{u}(P,t) dD \quad (2.49)$$

It is noted that distributed sensors are needed to obtain the displacements $u(P,t)$ and velocities $\dot{u}(P,t)$.

Implementation of IMSC using discrete activators and sensors

The implementation of IMSC requires distributed control, i.e. Control forces are applied at every point of the structure, and also requires distributed sensors, i.e. the displacements and velocities are measured at every point. This is however not realizable in practice. Thus discrete actuators and discrete sensors are used instead.

Let us consider the problem of controlling N modes by means of discrete actuators. The actuator forces can be treated and distributed by writing

$$f(P,t) = \sum_{j=1}^N F_j(t) \delta(P-P_j) \quad (2.50)$$

substituting (2.50) into (2.8) yields

$$f_r(t) = \sum_{j=1}^N \phi_r(P_j) F_j(t) \quad (2.51)$$

Introducing the matrix B as

$$B = \begin{bmatrix} \phi_1(P_1) & \phi_1(P_2) & \dots & \phi_1(P_N) \\ \phi_2(P_1) & \phi_2(P_2) & \dots & \phi_2(P_N) \\ \vdots & \vdots & & \vdots \\ \vdots & \vdots & & \vdots \\ \phi_N(P_1) & \phi_N(P_2) & \dots & \phi_N(P_N) \end{bmatrix} \quad (2.52)$$

we obtain

$$f(t) = B F(t) \quad (2.53)$$

where

$$f(t) = [f_1 \ f_2 \ \dots \ f_N]^T \quad (2.54)$$

$$F(t) = [F_1 \ F_2 \ \dots \ F_N]^T \quad (2.55)$$

Suppose B is nonsingular, then the actual control vector F(t) can be synthesized from the generalized control vector f(t) by

$$F(t) = B^{-1} f(t) \quad (2.56)$$

Next let us assume there are m sensors capable of measuring displacements and velocities at the discrete points $P=P_k$ ($k=1,2,\dots,m$). Then from these measurements the entire displacement pattern $u(P,t)$ and velocity pattern $\dot{u}(P,t)$ can be estimated by using various interpolation functions. The structure of the IMSC scheme using discrete actuators and sensors is shown in Figure 2.

2.4 Evaluation of the control schemes

The design of the coupled modal control scheme is straight forward since it is simply a pole placement problem if the observation spillover is negligible. Indeed if we set $C_R=0$ in (2.4), then the eigenvalues of the composite system are the eigenvalues of $(A_C + B_C K_C)$; $(A_C - G_C C_C)$ and A_R due to block triangularity. There are several techniques such as in [15,16] that help the control designer to select K_C and G_C such that $A_C + B_C K_C$ and $A_C - G_C C_C$ have desired eigenvalues. The control spillover is represented by

$$\dot{x}_R(t) = A_R x_R(t) + B_R K_C [x_C(t) + e_C(t)] \quad (2.57)$$

Since $e_C(t)$ and $x_C(t)$ will decay to zero, the control spillover will cause unwanted excitations of the residual modes, but it cannot shift the residual mode frequencies. Consequently the control spillover results in some

unwanted oscillations of the residual modes. So when the observation spillover is absent, then the control spillover degrades the system responses but cannot destabilize the system.

When observation spillover exists, then instability may occur when some of the eigenvalues of the composite system (2.40) are unstable.

The control and observation spillover can be minimized if the actuators and sensors are located at (or very near to) the zero of the mode shapes of the residual modes. This concept is limited since it creates uncontrollable and unobservable triple (A_C, B_C, C_C) that hinders the design of state estimators and state feedback laws. In addition, the freedom to locate sensors and actuators arbitrarily is rarely available to the designer since these locations are often already determined by structural considerations.

It is well known [12] that the IMSC scheme is capable of eliminating control and observation spillover. However it requires the implementation of distributed actuators and distributed sensors that unfortunately cannot be provided by the current state-of-the-art. Consequently, discrete actuators and discrete sensors have to be used. A question that is still not clearly answered is how many discrete actuators and sensors are necessary for a successful implementation of the IMSC scheme. In addition, the IMSC scheme when being implemented by discrete actuators also has control spillover into the uncontrolled modes. However as pointed out in [12], the control spillover effect is not very important.

Both control schemes, the coupled modal control and the IMSC require that a closed-form solution of the eigenvalue problem exist. Unfortunately the vast majority of continuous systems leads to eigenvalue problems that do not have closed-form solutions, owing to nonuniform mass or stiffness

distributions. Hence in this case, it is necessary to seek approximate solutions of the eigenvalue problem.

3. Modeling of the Polar Platform

One of the project activities is to obtain a model for a generic polar platform whose physical parameters are given in Table 1.

A NASTRAN finite element analysis package (McNeal Schwendler version) was employed to model the platform and its appendages by 52 nodes. The model is illustrated in Figure 3. The platform itself was modeled by 28 nodes, the solar panel and the astromast by 16 nodes and the engineering module by 8 nodes.

In the developed model, the payload carried by each module was assumed to be distributed uniformly throughout all nodes. Also the engineering module was assumed to be very rigid as compared to the platform or the solar panel.

The model considers only those degrees of freedom of the platform that contribute to its bending and torsional vibrations.

Table 2 lists the first ten modes of vibrations. The first two natural frequencies are the first rigid body modes in pitching and rolling. The remaining modes are the flexible modes of the platform.

It can be seen that the flexible modes are very low and highly condensed over a narrow band between 0.054Hz and 0.448 Hz. A sample of the first three modes of vibrations are shown in Fig. 4-6.

4. Project Research Results

In this section we will present some research results obtained by the principal investigators during the research period stated in the summary.

One of the project objectives is to evaluate several candidate control

schemes in order to select the most appropriate control scheme for the LFSS. The study of coupled-modal control and Independent Modal Space Control involves in such problems as pole allocation, eigenvalue assignment, state estimator design, canonical transformation etc. During the investigation of the above topics, some results have been found and are summarized below.

4.1 Canonical Transformation

Canonical transformation has been proven to be very useful in the design of state estimators and state feedback. In [14] two canonical transformations were developed for a class of time-varying multivariable control systems. Since most physical systems such as LFSS are time-varying in nature, this type of time-varying canonical transformations will be very helpful in design of more practical control schemes for LFSS.

4.2 Eigenvalue Assignment and Pole Allocation

The eigenvalue assignment or pole allocation problem is very essential to the control of LFSS since it is related to the system stability. Two common problems in control system design for LFSS are the selection of a state feedback gain to shift the natural modes of the LFSS to a set of desired damping modes, and the design of a state estimator whose eigenvalues can be arbitrarily assigned. These two problems can be treated as eigenvalue assignment or pole allocation problems. In [16] it was shown that eigenvalues can be arbitrarily assigned to a class of time-varying multivariable systems. Canonical transformation developed in [14] was employed to design the state feedback gain. The distributed control problem was considered in [17] where a control scheme was developed to arbitrarily allocate closed-loop poles to a distributed time-invariant system that is controlled by several pairs of sensors and actuators.

4.3 State Estimator Design

State estimator design is very crucial to the control of LFSS since the controlled state vector has to be estimated for the coupled modal control case and the modal state for the IMSC case. In [18] a new algorithm was proposed to design reduced-order state estimators for a class of time-varying multivariable control systems that are uniformly observable. The result in [18] is an extension of that in [15] where a full-order state estimator was designed.

4.4 Simulation of Control Schemes

Since the generic polar platform is relatively a complicated structure, we start the study of the control scheme by considering the control of a simply supported beam with one actuator and one sensor. Complete understanding of the control of this simply supported beam will help us to gain some insight of the control of the complete structure. The beam dynamics are modelled by the Euler-Bernoulli partial differential equation

$$m \frac{\partial^2}{\partial t^2} u(x,t) + EI \frac{\partial^4}{\partial x^4} u(x,t) = f(x,t) \quad (4.1)$$

For simplicity we set the mass m , the moment of inertia I , the modulus of elasticity E and the length of the beam to unity. The boundary conditions for this simply supported beam are

$$u(0,t) = u(1,t) = 0 \quad (4.2)$$

$$-\frac{\partial^2}{\partial x^2} u(0,t) = -\frac{\partial^2}{\partial x^2} u(1,t) = 0 \quad (4.3)$$

The eigenvalue solutions for this case are

$$\omega_k = (k\pi)^2 \quad (4.4)$$

and

$$\phi_k = \sin(k\pi x) \quad (4.5)$$

The beam is controlled by a single point actuator at $x = 1/6$:

$$f(x,t) = (1/2)^{.5} \delta(x - 1/6) f(t) \quad (4.6)$$

and the displacement is measured by a single point sensor located at $x = 5/6$:

$$y(t) = u(5/6,t) \quad (4.7)$$

Using the Matlab and the control tool box software package, an active controller was designed to control the first three modes of the beam. To minimize the following unweighted energy

$$J = \int_0^{\infty} [E(t) + 0.1f^2(t)]dt \quad (4.8)$$

where

$$E(t) = 1/2 \sum_{k=1}^3 (\omega_k^2 u_k^2 + \dot{u}_k^2) \quad (4.9)$$

the control gain was determined to be

$$K_C = [-3.87 \quad -3.86 \quad -3.86 \quad -1.01 \quad -6.08 \quad -20.3] \quad (4.10)$$

A state estimator was designed to estimate the controlled modes. The state estimator gain G_C given below:

$$G_C = [711.8 \quad 52.34 \quad -7.39 \quad 10.06 \quad -5.97 \quad 1.98]^T \quad (4.11)$$

will assign stable eigenvalues to the state estimator. Several simulation runs were made to study the performance of the active controllers and the effect of the control and observation spillover.

In all simulation runs, an impulse disturbance was created to excite the system. Figures 8 and 9 present the effects of control and observation spillover. We note that when spillover exists, the displacement did not reach the zero steady state. It has an oscillation with small amplitude caused by control spillover into the uncontrolled modes. Even though the observation exists in this case, the system is still stable. Fig. 10 and 11 display the sensor output and actuator input when no spillover exists. We notice that the displacement was decayed to zero. The control spillover into the 4th and 5th uncontrolled modes is illustrated in Fig. 12 and 13, respectively. The eigenvalues of the composite system [Equation (2.40)] for all possible cases of spillover are given in Table 2a. Table 2b shows the eigenvalues of the closed-loop system, the state estimator, controlled subsystem and uncontrolled subsystem.

In Table 3a we note that when no observation spillover exists, the eigenvalues of the composite system consist of the eigenvalues of the closed-loop system, the state estimator, and the uncontrolled subsystem. This agrees with the discussion made in Section 2.3.

5. Current and Future Research

Continuing the research stated in Section 4, we currently focus on the study of spillover minimization. As we have seen, the system simulation results showed that the system performance is degraded at the presence of control spillover. The LFSS can also become unstable if the observation

spillover exists. Therefore spillover minimization study is very crucial to the control of LFSS. We are investigating the minimization of the spillover by

- (a) Proper locating of actuator and sensors.
- (b) Determining a sufficient number of actuators and sensors needed.
- (c) Applying the IMSC method to the generic polar platform.

The above study is carried out mostly by simulating the system for various situations using system simulation languages in order to set up a guideline for selecting and locating actuators and sensors.

After the control of the simply-supported beam has been studied throughout, we will apply the resulting control scheme to the complete generic polar platform. Several control issues such as given below should be addressed in the future research:

- (a) Evaluation of the application of coupled-modal control and IMSP to the generic polar platform in terms of feasibility, reliability, spillover, and computational effort.
- (b) Implementation of an adaptive control scheme for the system.
- (c) Study of a robust controller when the system parameters are not well-known and when unpredictable disturbances are expected.

6. Conclusion

In this report we first updated the research related to project. The modelling of the generic polar platform using finite element method was discussed. We then presented some preliminary results of the control system study using computer simulation and some theoretical research results of such problems as eigenvalues, state estimator, and state feedback design. Current research effort was discussed and future research activities were assessed.

References

1. M.J. Balas, "Active Control of Flexible Systems," J. Optimization Theory and Applications, Vol. 25, No. 3, pp 415-436, July 1978.
2. M.J. Balas, "Trends in Large Space Structure Control Theory: Fondest Hopes, Wildest Dreams," IEEE Trans. Automat. Control., AC - 27, No. 3, pp. 522-534, June 1982.
3. Michel A. Floyd, "Comment on a Comparison of Control Techniques for Large Flexible Systems," J. of Guidance and Control, Vol. 7, No. 5, pp. 634-635, 1984.
4. A. L. Hale and G. A. Rahn, "Robust Control of Self - Adjoint Distributed - Parameter Structures," J. of Guidance and Control, Vol. 7, No. 3, pp. 263-273, 1984.
5. P. C. Hughes and R. E. Skelton, "Controllability and Observability for Flexible Spacecraft," J. of Guidance and Control, Vol. 3, pp. 452-459, Oct. 1980.
6. D. J. Inman, "Modal Decoupling Conditions for Distributed Control of Flexible Structures," J. of Guidance and Control, Vol. 7, No. 6, pp. 750-752, 1984.
7. T. L. Johnson, "Progress in Modelling and Control of Flexible Spacecraft," Journal of the Franklin Institute, Vol. 315, No. 516, pp. 495-520, May/June 1983.
8. S. Kumar and J. H. Seinfeld, "Optimal Location of Measurements for Distributed Parameter Estimation," IEEE Trans. Automat. Control, AC - 23, No. 4, pp. 690-698, Aug. 1978.
9. L. Meirovitch, and H. Baruh, "On the problem of observation spillover in Distributed - Parameter Systems," Journal of Optimization Theory and Applications, Vol 39, No. 2, pp. 611-620.
10. L. Meirovitch and H. Baruh, "Control of Self-Adjoint Distributed - Parameter Systems," J. of Guidance and Control, Vol. 5, No. 1, pp. 60-66, Feb. 1982.
11. L. Meirovitch and H. Oz, "Modal Space Control of Distributed Gyroscopic Systems," J. of Guidance and Control, Vol. 3, No. 2, pp. 140-150, April 1980.
12. L. Meirovitch and others, "A Comparison of Control Techniques for Large Flexible Systems," J. of Guidance, Control, and Dynamics, Vol. 6, pp. 302-310, July - Aug. 1983.
13. L. Meirovitch and H. Baruh, "The Implementation of Modal Filters for

Control of Structures," J. of Guidance and Control, Vol. 8, No. 6, pp. 707-716, Dec. 1985.

14. C. C. Nguyen, "Canonical Transformation for a class of Time - Varying Multivariable Systems," Int. J. Control, Vol. 43, No. 4, pp. 1061-1074, April 1986.
15. C. C. Nguyen, "Design of State Estimator for a Class of Time-Varying Multivariable Systems," IEEE Trans. Automat. Control, AC-30, Feb. 1985.
16. C. C. Nguyen, "Arbitrary Eigenvalue Assignments for Linear Time-Varying Multivariable Control Systems," to appear in Int. Journal of Control, 1987.
17. C. C. Nguyen, "Pole Allocation for Decentralized-Control Systems," Proc. Int. Conf. Modelling and Simulation, AMSF, Williamsburg, Sept. 1986.
18. C. C. Nguyen, "Design of Reduced - Order State Estimators for Linear Time - Varying Multivariable Systems," submitted for publication in Int. Journal of Control, 1986.
19. D. Schaechter, "Distributed Control of Large Space Structures," Jet Propulsion Lab Report, #81-15, May 1981.
20. D. Turner and H. M. Chun, "Optimal Distributed Control of a Flexible Spacecraft During a Large - Angle Maneuver," J. of Guidance, Control, and Dynamics, Vol. 7, No. 3, pp. 257-264, 1984.
21. S. Omatu, "Optimization of Sensor and Actuator Locations in a Distributed Parameter System," Journal of the Franklin Institute, Vol. 315, No. 516, pp. 407-421, May/June 1983.
22. H. Oz, and others, "Some Problems Associated with Digital Control of Dynamical Systems," J. of Guidance and Control, Vol. 3, No. 6, pp. 523-528, Dec. 1980.
23. W. E. Vander Velde, and C. R. Cariguau, "Number and Placement of Control System Components Considering Possible Failures," Journal of Guidance and Control, Vol. 7, No. 6, pp. 703-709, Dec 1984.
24. M. Abdel - Rohman and H. H. Leipholz, "Automatic Active Control of Structures," Journal of the Structural Division, pp. 663-677, March 1980.
25. G. S. West - Vukovich et al, "The Decentralized Control of Large Flexible Space Structures," IEEE Trans. Automatic Control, Vol. AC-29, No. 10, pp. 866-879, Oct. 1984.

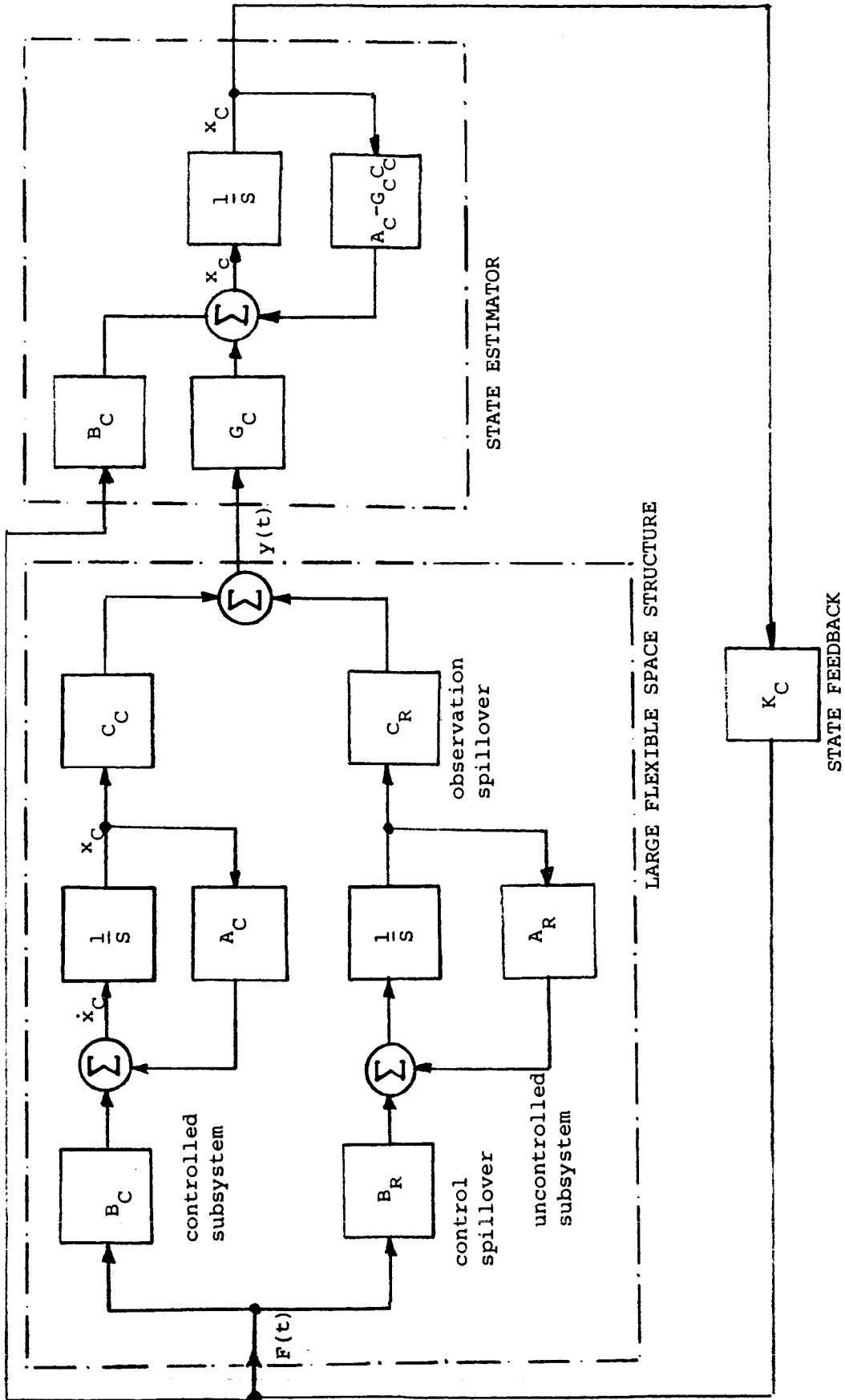


FIGURE 1: The Structure of the Coupled Modal Control

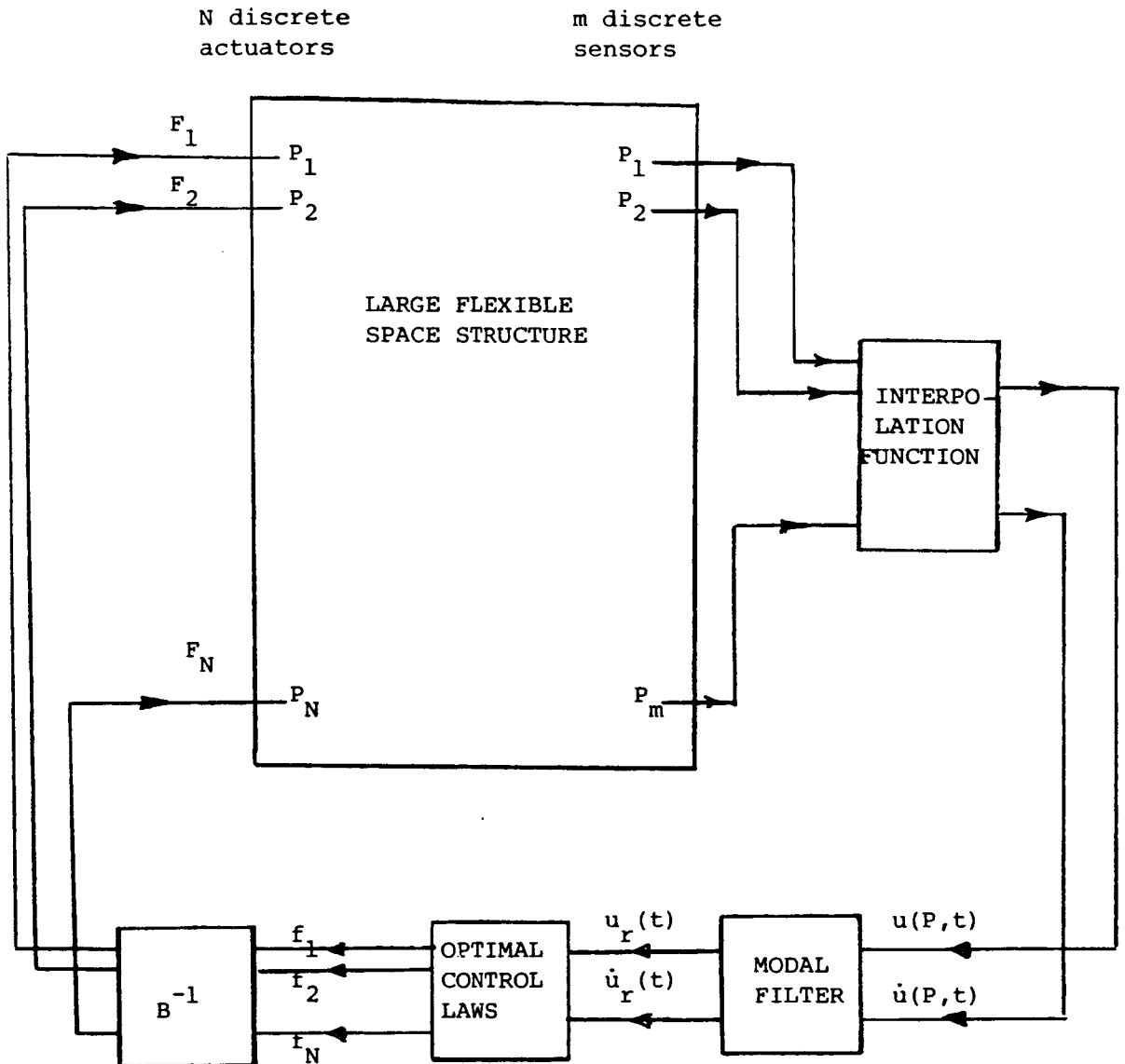


FIGURE 2: The Structure of the Independent Modal Space Control

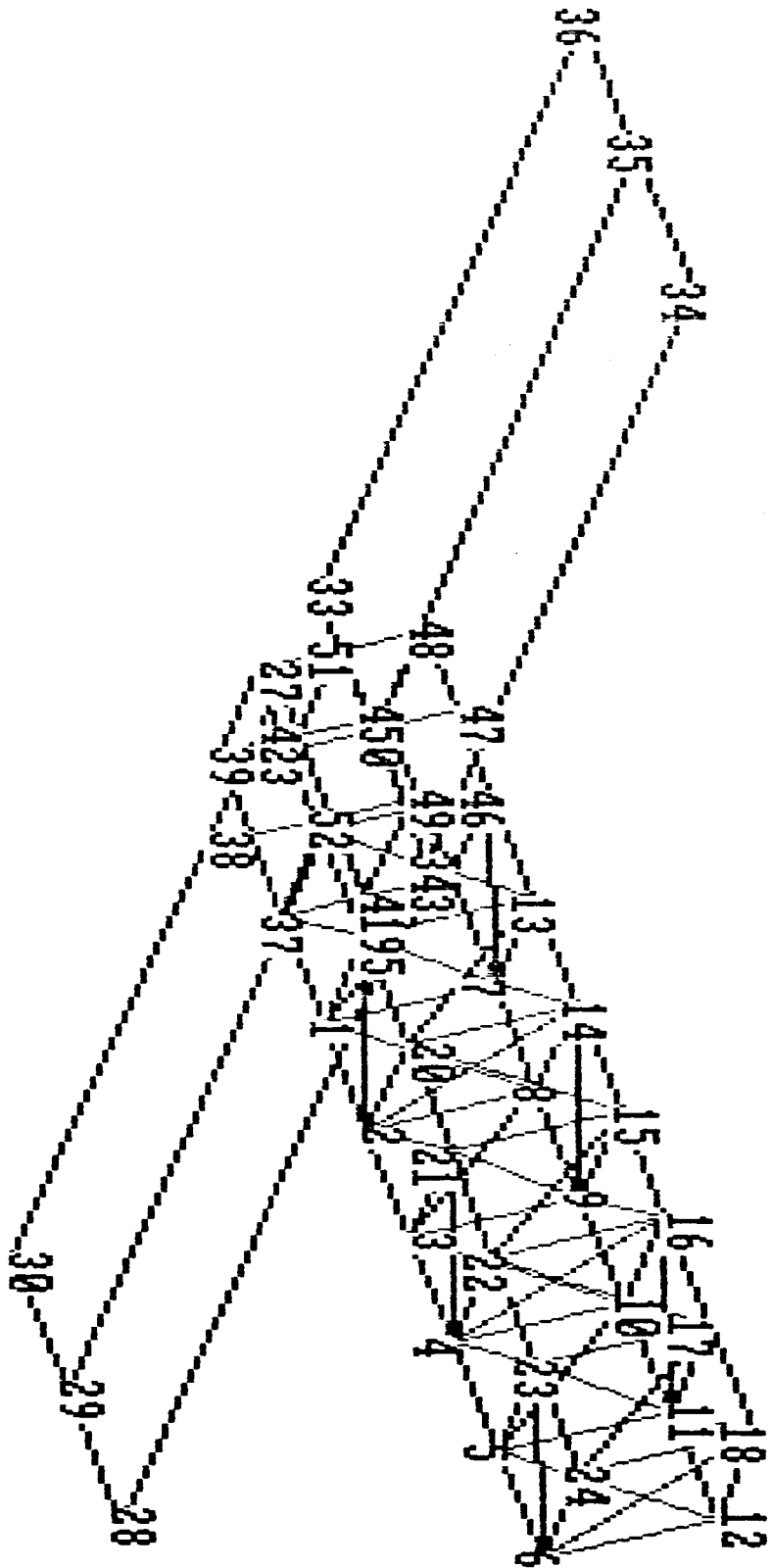


FIGURE 3: The Finite Element Model of the Generic Polar Platform

MODE 1 (0 HZ)

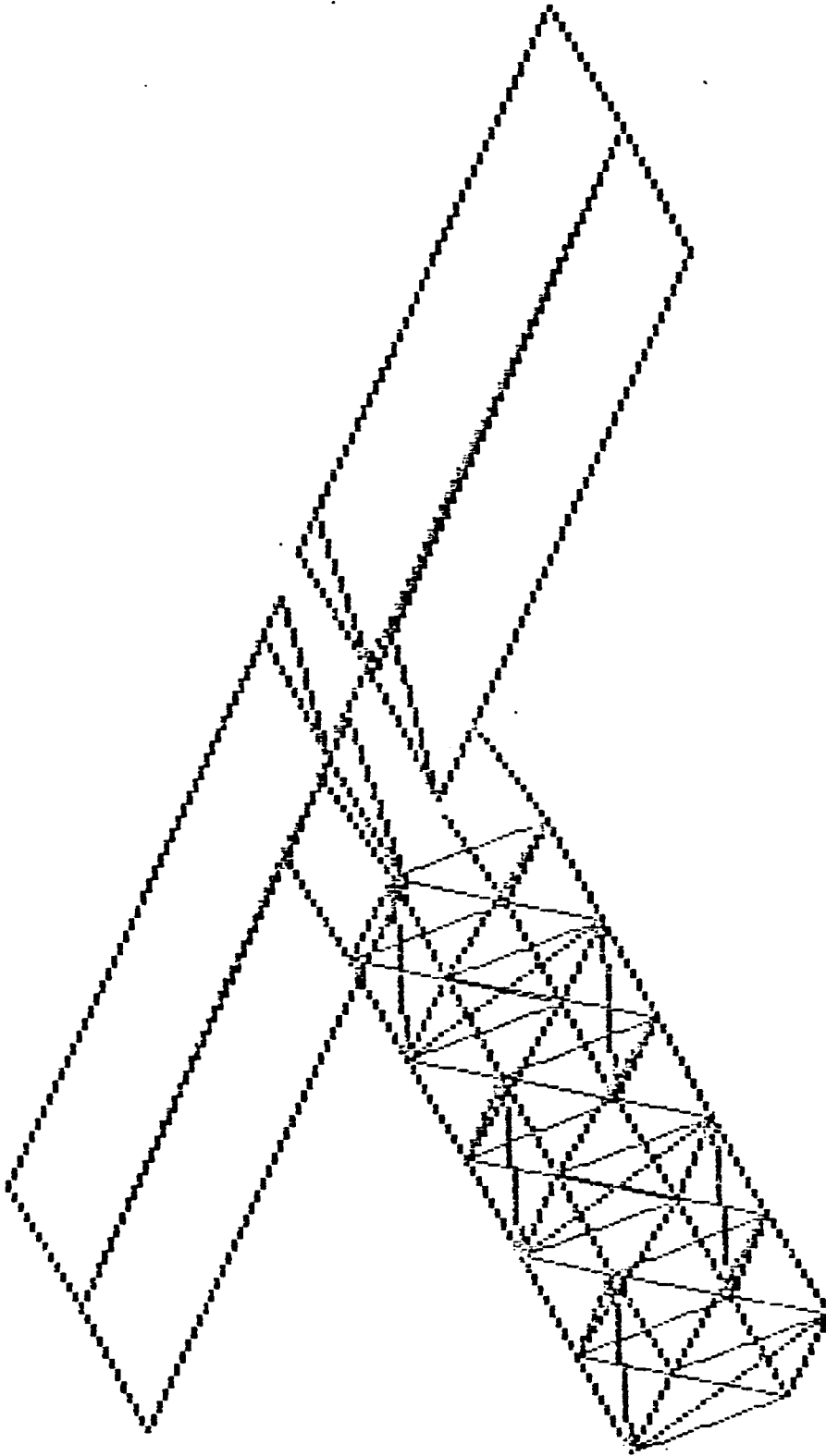


FIGURE 4: The First Mode of Vibration

MODE 2 (0 HZ)

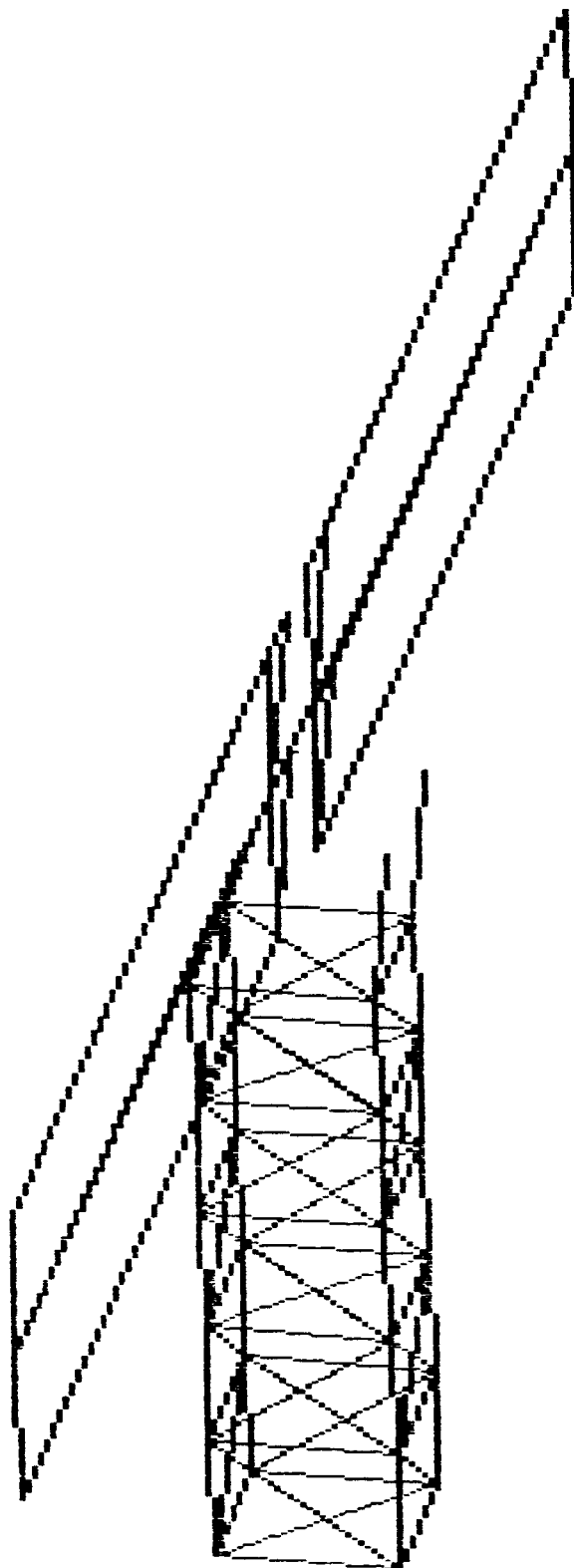


FIGURE 5 : The Second Mode of Vibration

MODE 3 (9.0545 HZ)

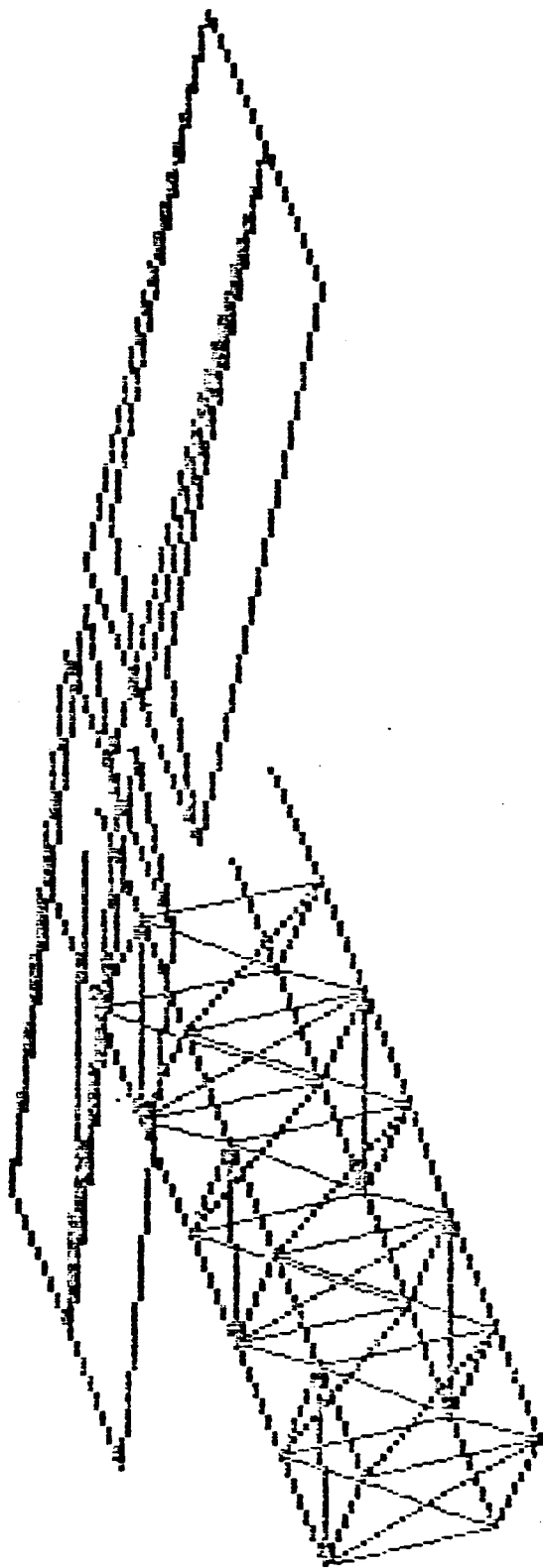


FIGURE 6: The Third Mode of Vibration

MODE 4 (9.089 HZ)

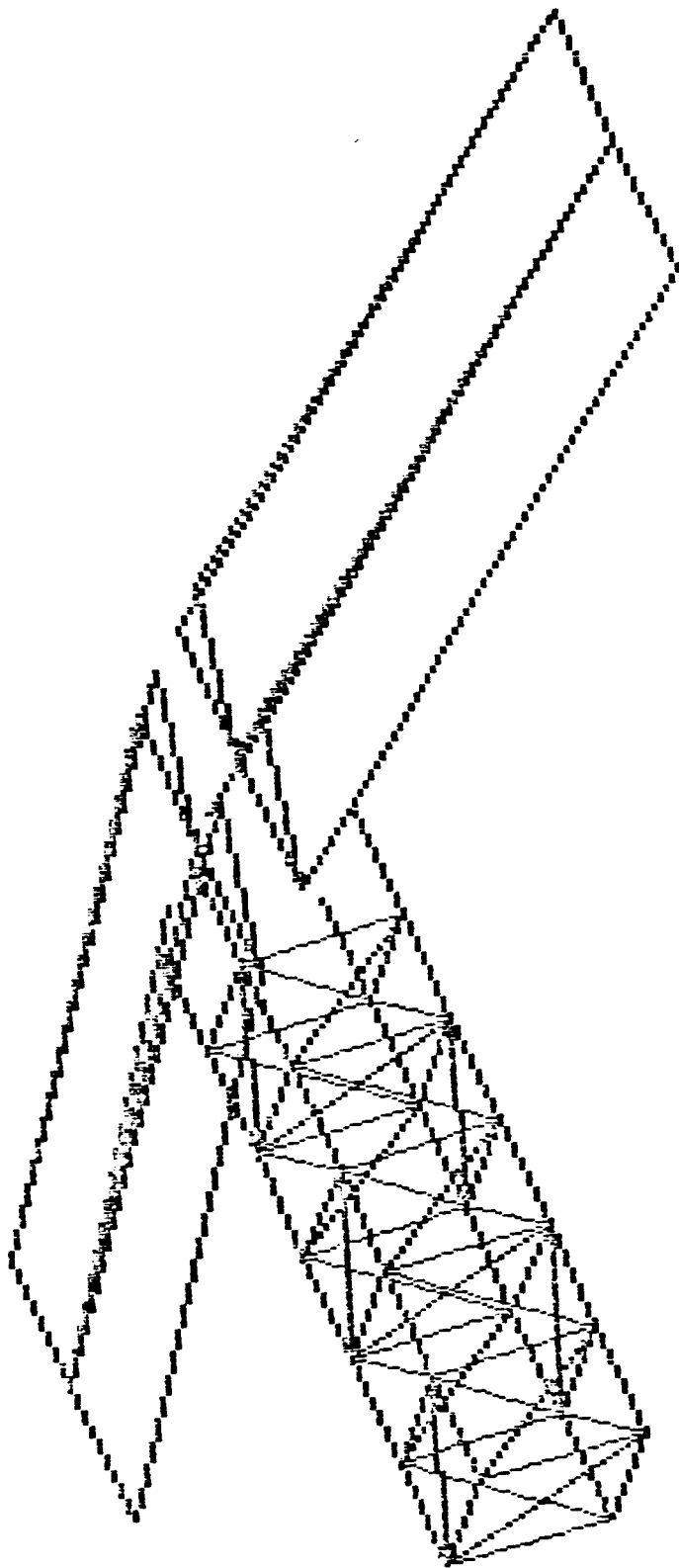


FIGURE 7: The Fourth Mode of Vibration

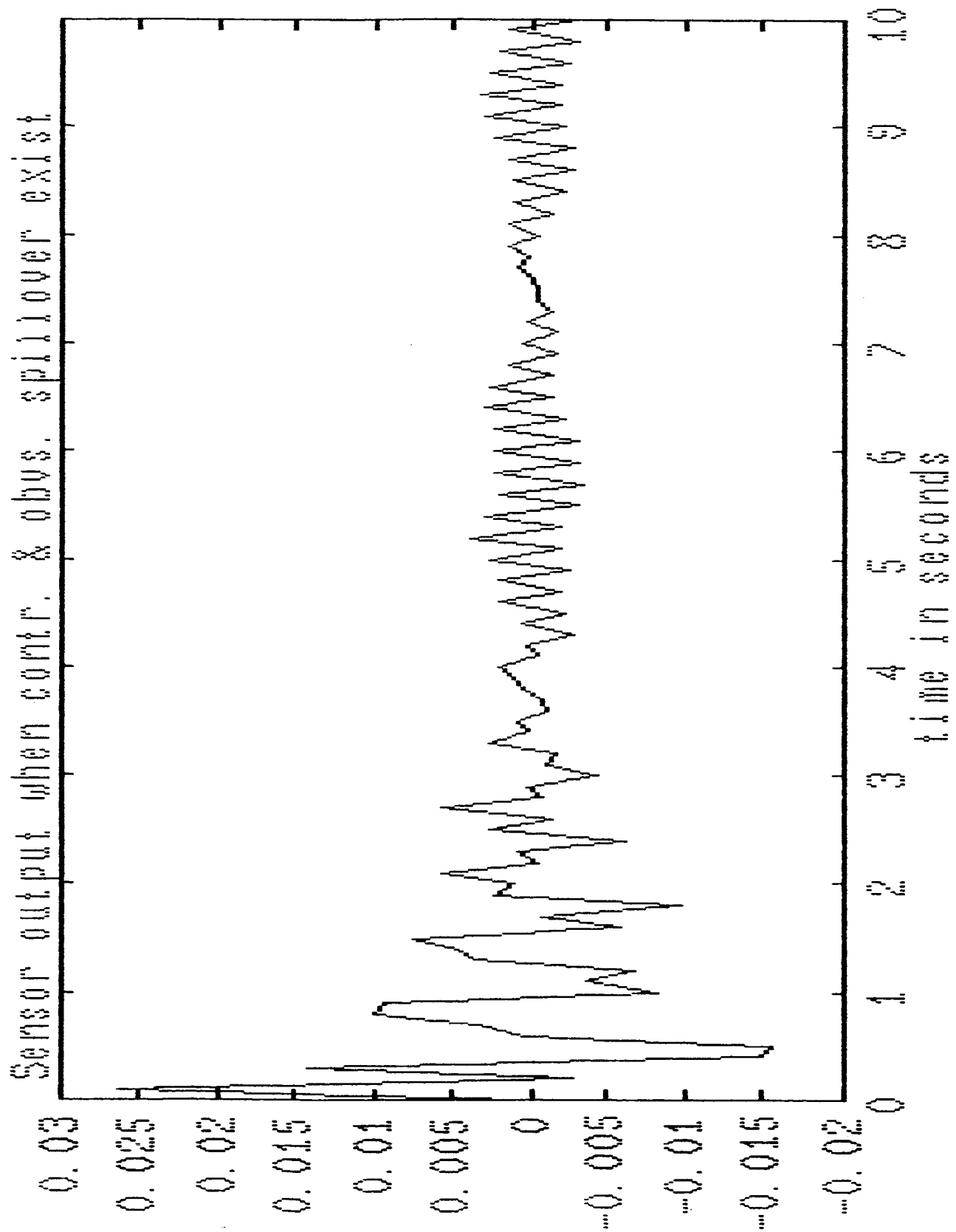


FIGURE 8: The Sensor Output when the Control and Observation Spillover exist

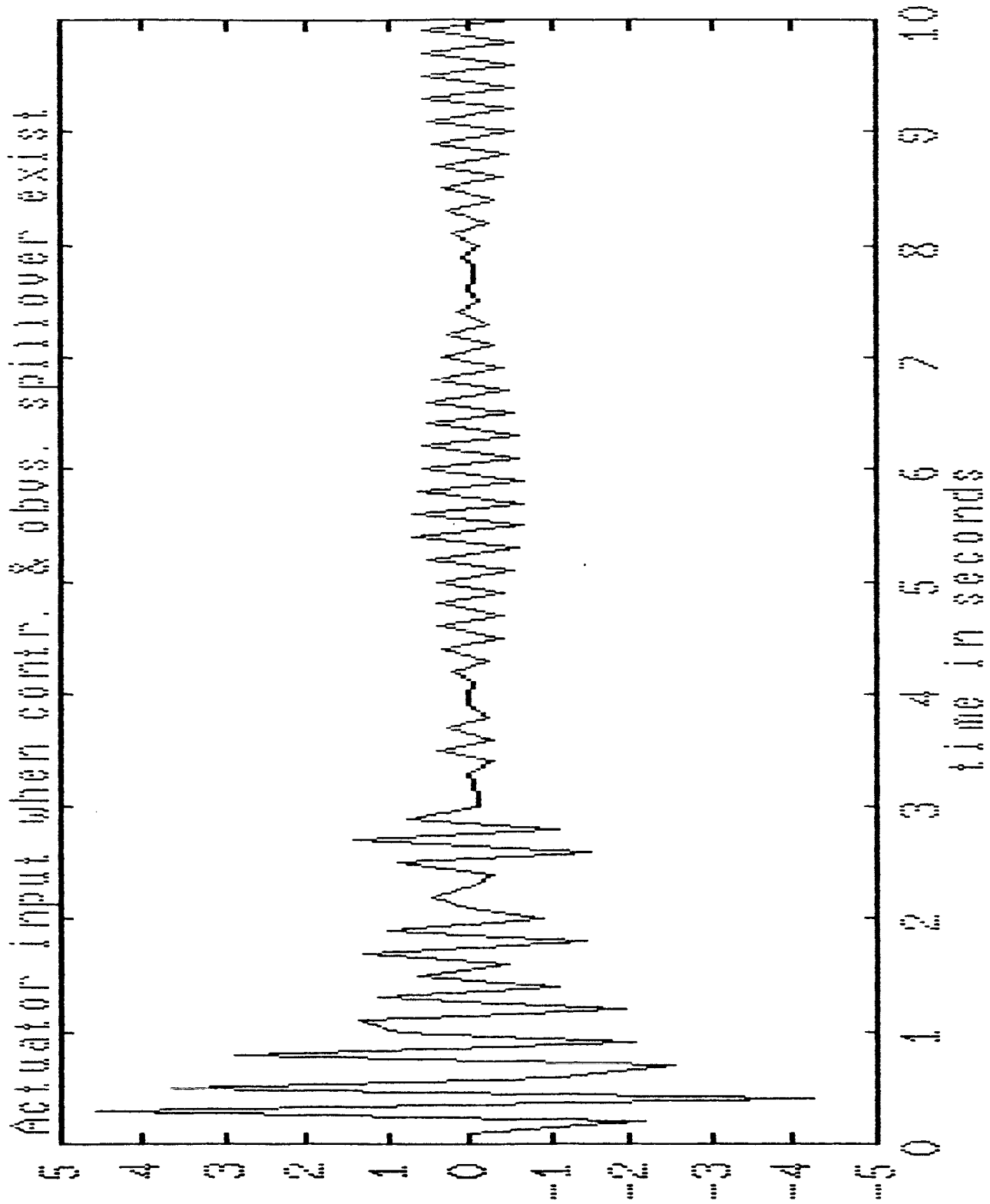


FIGURE 9: Actuator Input at the Presence of the Control Spillover and Observation Spillover

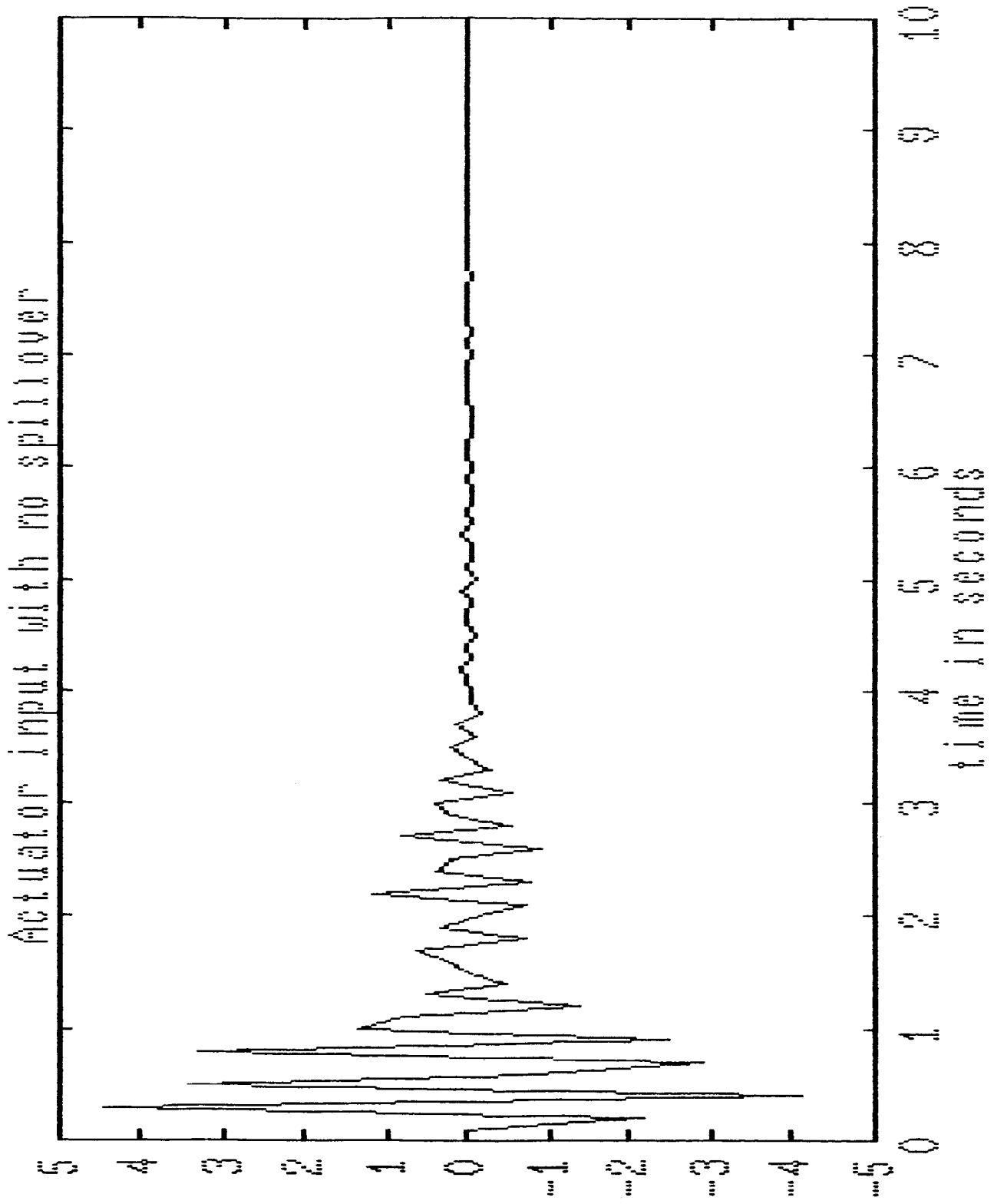


FIGURE 10: Actuator Input with no Control and Observation Spillover

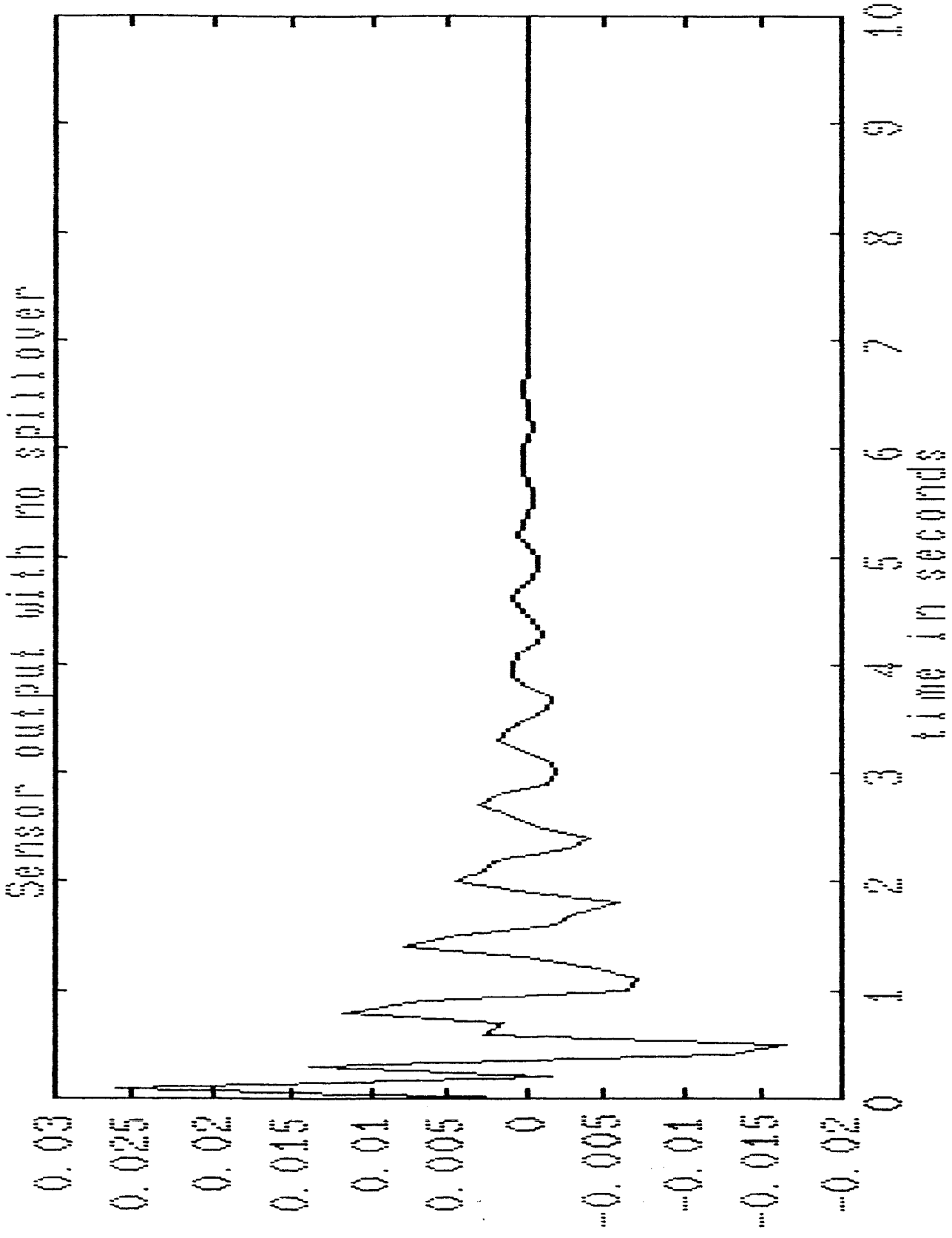


FIGURE 11: Sensor Output with no Control and Observation Spillover

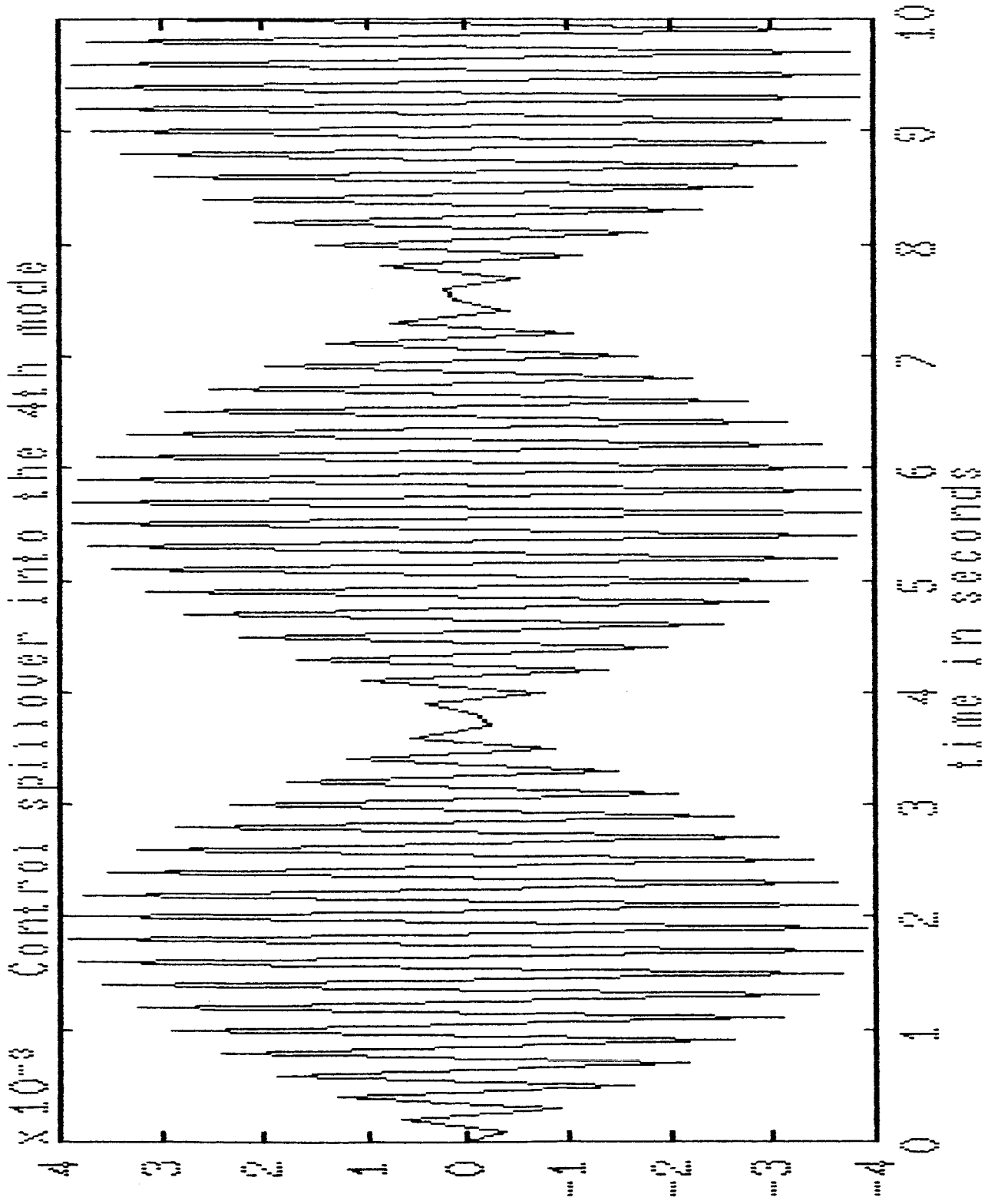


FIGURE 12: Control Spillover into the 4th Mode

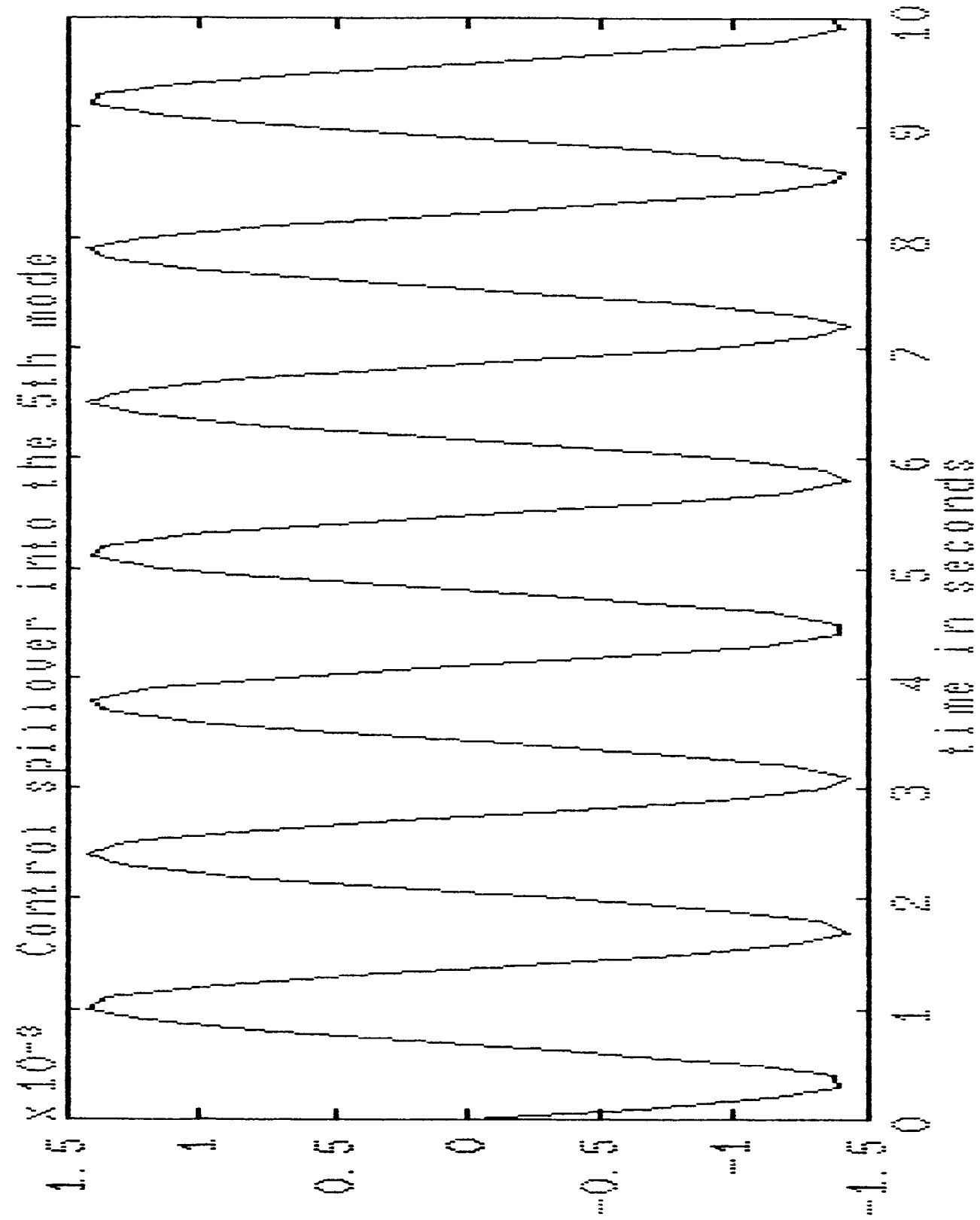


FIGURE 13: Control Spillover into the 5th Mode

PARAMETER	VALUE
OVERALL LENGTH OF THE PLATFORM	45 ft
PLATFORM WIDTH	6 ft
PLATFORM HEIGHT	6 ft
LENGTH OF SOLAR ARRAY	60 ft
WIDTH OF SOLAR ARRAY	15 ft
NUMBER OF MODULES	6
MASS/MODULE	600.00 kg
LENGTH OF ENGINEERING MODULE	9 ft
HEIGHT OF ENGINEERING MODULE	6 ft
MASS OF ENGINEERING MODULE	5000.00 kg
LENGTH OF STRUCTURAL MEMBERS	6 ft
STRUCTURAL MEMBER OUTER DIAMETER	1 in.
STRUCTURAL MEMBER INNER DIAMETER	0.875 in.
STRUCTURAL MEMBER MATERIAL	Aluminium
DESITY OF THE ASTROMAST SUPPORTING THE SOLAR ARRAY	2.2 kg/ft
ASTROMAST FLEXURAL RIGIDITY	$15.20 \times 10^6 \text{ lb in}^2$
ASTROMAST TORSIONAL RIGIDITY	5 $\times 10^6 \text{ lb in}^2$

TABLE 1: Physical Parameters of the Generic Polar Platform

MODE	frequency in Hz
1	0
2	5.397×10^{-6}
3	5.457×10^{-2}
4	8.956×10^{-2}
5	1.404×10^{-1}
6	3.635×10^{-1}
7	3.837×10^{-1}
8	4.190×10^{-1}
9	4.301×10^{-1}
10	4.488×10^{-1}

TABLE 2: The First Ten Modes of Vibrations

ORIGINAL PAGE IS
OF POOR QUALITY

w/contr.& ob. spill.	w/o contr.& ob. spill.	no ob. spillover	no contr. spill.
1.0E+002 *			
0.0000 + 2.4674i	-0.0137 + 0.8883i	-0.0137 + 0.8883i	-0.0000 + 2.4674i
0.0000 - 2.4674i	-0.0137 - 0.8883i	-0.0137 - 0.8883i	-0.0000 - 2.4674i
-0.0003 + 1.5791i	-0.0101 + 0.8864i	-0.0101 + 0.8864i	0.0000 + 1.5791i
-0.0003 - 1.5791i	-0.0101 - 0.8864i	-0.0101 - 0.8864i	0.0000 - 1.5791i
-0.0139 + 0.8886i	-0.0170 + 0.2185i	-0.0170 + 0.2185i	-0.0101 + 0.8864i
-0.0139 - 0.8886i	-0.0170 - 0.2185i	-0.0170 - 0.2185i	-0.0101 - 0.8864i
-0.0099 + 0.8862i	-0.0068 + 0.0988i	-0.0068 + 0.0988i	-0.0137 + 0.8883i
-0.0099 - 0.8862i	-0.0068 - 0.0988i	-0.0068 - 0.0988i	-0.0137 - 0.8883i
-0.0167 + 0.2186i	-0.0118 + 0.3948i	-0.0118 + 0.3948i	-0.0068 + 0.0988i
-0.0167 - 0.2186i	-0.0118 - 0.3948i	-0.0118 - 0.3948i	-0.0068 - 0.0988i
-0.0068 + 0.0988i	-0.0339 + 0.3815i	-0.0339 + 0.3815i	-0.0170 + 0.2185i
-0.0068 - 0.0988i	-0.0339 - 0.3815i	-0.0339 - 0.3815i	-0.0170 - 0.2185i
-0.0339 + 0.3814i	0 + 1.5791i	0 + 1.5791i	-0.0339 + 0.3815i
-0.0339 - 0.3814i	0 - 1.5791i	0 - 1.5791i	-0.0339 - 0.3815i
-0.0118 + 0.3949i	0 + 3.5531i	0 + 3.5531i	-0.0118 + 0.3948i
-0.0118 - 0.3949i	0 - 3.5531i	0 - 3.5531i	-0.0118 - 0.3948i
-0.0000 + 3.5531i	0 + 2.4674i	0 + 2.4674i	0 + 3.5531i
-0.0000 - 3.5531i	0 - 2.4674i	0 - 2.4674i	0 - 3.5531i

TABLE 3a: Eigenvalues of the Composite System

closed-loop system	state estimator	control. subsystem	uncontr. subsys.
1.0E+002 *			
-0.0137 + 0.8883i	-0.0101 + 0.8864i	0 + 0.0987i	0 + 1.5791i
-0.0137 - 0.8883i	-0.0101 - 0.8864i	0 - 0.0987i	0 - 1.5791i
-0.0118 + 0.3948i	-0.0170 + 0.2185i	0 + 0.8883i	0 + 3.5531i
-0.0118 - 0.3948i	-0.0170 - 0.2185i	0 - 0.8883i	0 - 3.5531i
-0.0068 + 0.0988i	-0.0339 + 0.3815i	0 + 0.3948i	0 + 2.4674i
-0.0068 - 0.0988i	-0.0339 - 0.3815i	0 - 0.3948i	0 - 2.4674i

TABLE 3b: Eigenvalues of the Closed-Loop System, State Estimator, Controlled Subsystem, and Uncontrolled Subsystem